Multiscale study of charge mobility of organic semiconductor with dynamic disorders

Linjun Wang,[a] Qikai Li,[a] Zhigang Shuai,*[ab] Liping Chen[c] and Qiang Shi[c]

Received 2nd July 2009, Accepted 18th January 2010
First published as an Advance Article on the web 22nd February 2010
DOI: 10.1039/b913183c

The impact of dynamic disorder arising from the thermal fluctuations on the charge transport in organic semiconductors is studied by a multi-scale approach combining molecular dynamics, electronic structure calculations and kinetic Monte Carlo simulations for pentacene crystal of thin-film phase. It is found that for 1-D arrays, such fluctuations severely reduce charge mobility as temperature increases. However, when going from an 1-D array to an 2-D herringbone layer, for a wide range of temperatures, the charge transport property is found to be unaffected by such disorders from our multiscale computational study. And in some extreme cases, when the fluctuations of the hopping integral are even larger than their average values, the dynamic disorders can increase the charge mobility. In addition, we point out that the "band-like" behavior concluded by the experiment can be reproduced by quantum charge transfer involving nuclear vibration tunneling effects within a hopping model.

I. Introduction

With the rapid development of new materials for application in organic electronics,[1–3] the charge transport mechanism in organic semiconductors has been of great interest recently.[4–7] The experimental evidence based on single crystals has shown that the intrinsic charge mobility normally decreases with temperature.[8–12] In inorganic materials, this kind of "band-like" transport is widely described using the standard band theory, in which the charge is delocalized over the crystal and scattered by phonons. However, since organic molecules are held together by weak interactions, the delocalized picture of band theory is unlikely in organic materials due to (i) the small intermolecular transfer integrals which result in narrow bandwidth and the mean free path of charge carriers becomes shorter than the lattice constant at high temperatures;[13] and (ii) the strong thermal fluctuation of transfer integrals which destroys the translational symmetry of the electronic Hamiltonian.[14] The latter, *i.e.*, the dynamic disorder of transfer integrals, also known as the nonlocal electron–phonon coupling,[15] has been studied in detail within the small polaron model and has shown a dominant role for the temperature dependence of charge mobility.[16] However, the thermal average approximation in the similarity transformation for the many-body expansion in the small polaron theory has to be employed which smears out the fluctuation nature, and the perturbative treatment of the transfer integrals limits its application range.[16–18] The impact of the dynamic disorder on charge transport within the localized charge hopping model is still unclear.

Recently, Troisi *et al.* observed numerically the time evolution of transfer integrals in organic crystals by means of molecular dynamics (MD) and quantum chemistry,[19] based on which a disorder-limited transport mechanism was proposed to explain the "band-like" temperature dependence of mobility in pentacene through solving the time-dependent Schrödinger equation for a 1-D molecular array.[14] We notice that the scaling theory in the case of static disorder shows that the localization of the electronic states depends strongly on the dimensions.[20,21] Whether the disorder-limited mechanism still survives in real 3-D materials is yet to be established. In fact, Nan *et al.* found that the charge transfer rates between neighboring molecules are independent of temperature below room temperature due to the nuclear tunneling effects arising from carrier coupling with high-frequency intra-molecular modes, and thus result in a "band-like" behavior in mobility for a wide range of temperatures.[22] Thus, it is of great interest to study the different roles of dynamic disorder and nuclear tunneling effect on the "band-like" transport behavior.

In this study, our primary interest is to reveal the impact of dynamic disorder on charge transport in higher than one dimension. We choose the thin film phase of the pentacene crystal with a typical layer-by-layer structure and focus on the intra-layer hole transport properties. The inter-layer electronic coupling is generally weak in comparison with intra-layer electronic couplings in molecular crystals,[23] and has negligible influence on the charge transport within the intra-layer plane. Therefore, the present work only deals with 1-D and 2-D charge transport properties. This thin-film phase is a substrate-induced polymorph, commonly existing in pentacene thin-film transistors with hole mobility exceeding 5.0 cm^2/Vs,[24] and has thus received a lot of attention in literature.[25–27] We perform MD simulations to achieve the time evolution of molecule geometries, and quantum chemical calculations for the transfer

[a] *Key Laboratory of Organic Solids, Beijing National Laboratory for Molecular Science, Institute of Chemistry, Chinese Academy of Sciences, 100190 Beijing, P R China. Fax: +86 10 6252 5573; Tel: +86 10 6252 1934*
[b] *Department of Chemistry, Tsinghua University, 100084 Beijing, P R China. E-mail: zgshuai@tsinghua.edu.cn*
[c] *Key Laboratory of Structural Chemistry for Unstable and Stable Species, Institute of Chemistry, Chinese Academy of Sciences, 100190, Beijing, P R China*

integrals at each MD snapshot, then we apply the kinetic Monte-Carlo method[28] to simulate charge carrier diffusion, considering the electron transfer rate with the presence of dynamic disorder. Within the present multiscale method, we are also able to study the nuclear tunneling effect using disorder-free transfer integrals.

II. Theoretical methodology

A Tight-binding model

The basic model to describe charge transport in disordered systems is based on the tight-binding Hamiltonian:[5,29–31]

$$H = \sum_m \varepsilon_m |m\rangle\langle m| + \sum_{mn} V_{mn} |m\rangle\langle n| \qquad (1)$$

Here, m and n are site (molecule) indices and ε_m is the on-site energy (molecular frontier orbital energy) at site m, and V_{mn} is the transfer integral coupling two adjacent molecules m and n. The modulation of ε_m and V_{mn} by molecular vibrations is termed as the local and nonlocal electron–phonon coupling, respectively, and is dominant by the intra- and intermolecular vibrations, respectively.[16]

B Local electron–phonon coupling

The local electron–phonon coupling is often characterized by the Huang-Rhys factors through normal-mode analysis.[5,7,22] Within this approach, the geometries of neutral and charged molecules are first fully optimized quantum chemically and the normal modes are calculated at the equilibrium structures. Then the changes in geometry between the neutral and charged states are projected onto all the normal modes.[32] Finally, the Huang-Rhys factor related to the ith vibrational mode can be calculated by $S_i = 1/\hbar\omega_i \times k_i \Delta Q_i^2/2$, where ΔQ_i represents the rigid displacement projected onto the ith normal mode (Fig. 1), k_i and ω_i are the corresponding force constant and the circular frequency for the ith normal mode. In practice, the Huang-Rhys factors can be obtained through the DUSHIN program developed by Reimers.[32]

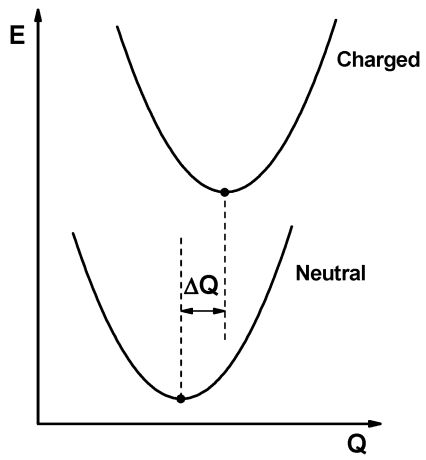

Fig. 1 Schematic representation of the potential energy surface of the neutral and charged molecules. ΔQ is the normal mode displacement.

C Nonlocal electron–phonon coupling

The nonlocal electron–phonon coupling in molecular crystals can be described by the time evolution of transfer integrals in a classical manner since it is mostly determined by the low frequency intermolecular vibrations and thereby the quantum effect is negligible at high temperatures.[16,19] The classical molecular dynamics simulations based on a supercell of molecules are performed and the transfer integrals are calculated at each snapshot.[19] In literature, there are a number of computational methods to get the transfer integral at fixed molecular dimer geometry, *e.g.*, the energy level splitting method,[33,34] the minimized energy level splitting along the reaction path method,[35] the direct evaluation method[36,37] and the site-energy corrected coupling method.[38] The benchmark study of the performance using these methods has been given elsewhere.[39] It has been found that the last three methods give very close results. In this work, the transfer integrals are calculated with the site-energy correction method:[38]

$$V_{mn} = \frac{V^0_{mn} - \frac{1}{2}(e_m + e_n)S_{mn}}{1 - S^2_{mn}} \qquad (2)$$

Here, $e_m = \langle \Phi_m | H | \Phi_m \rangle$, $V^0{}_{mn} = \langle \Phi_m | H | \Phi_n \rangle$, and $S_{mn} = \langle \Phi_m | S | \Phi_n \rangle$, where Φ_m and Φ_n are the highest occupied molecular orbitals (HOMOs) of the two molecules in the dimer which are responsible for the hole transport, H and S are the dimer Hamiltonian and the overlap matrices, respectively.

In this way, the time evolution of transfer integrals can be obtained as being calculated at each snapshot. Then a discrete Fourier transformation can be performed to the time-dependent transfer integral fluctuation: $\Delta V_{mn}(t) = V_{mn}(t) - \langle V_{mn} \rangle$. And the transfer integral $V_{mn}(t)$ can be expressed by

$$V_{mn}(t) = \langle V_{mn} \rangle + \sum_{k=0}^{N/2} \mathrm{Re}V_k \cos(\omega_k t + \varphi_0) + \sum_{k=0}^{N/2} \mathrm{Im}V_k \sin(\omega_k t + \varphi_0) \qquad (3)$$

where N is the total number of MD snapshots, $\mathrm{Re}V$ and $\mathrm{Im}V$ are the amplitudes of cosine and sine basis functions, on the basis of which the contributions of different phonons to the transfer integral fluctuation can be achieved. Besides, the same type of molecular dimer in the crystal should have the same thermal fluctuation property. Therefore, one can deal with a very small amount of typical dimers to get the Fourier coefficients, and the time-dependent transfer integral between all molecular dimers can be realized using eqn (3) with different phase factor φ_0. The phase factor can be chosen randomly because there is hardly any fluctuation correlation between transfer integrals of different pairs.[19]

D Charge transfer rate

The semiclassical Marcus theory has been widely used to calculate the electron transfer rate between a molecular dimer for room-temperature transport properties.[40–43] Considering that the nuclear tunneling effect should be important since the high frequency intramolecular modes are involved in the electron transfer process[5,16] and this effect gets even stronger at low temperatures,[22,44] we consider a general quantum-mechanical

charge transfer rate starting directly from the Fermi Golden Rule under the displaced harmonic oscillator approximation[45]

$$k = \frac{V^2}{\hbar^2}\int_{-\infty}^{\infty} \mathrm{d}t \exp\left\{ i\omega_{fi}t - \sum_j S_j[(2n_j+1) - n_j e^{-i\omega_j t} - (n_j+1)e^{i\omega_j t}] \right\} \quad (4)$$

Here, ω_{fi} goes to zero due to the self-exchange reaction character of the electron transfer between the same kind of molecules, $n_j = 1/(\exp(\hbar\omega_j/k_\mathrm{B}T) - 1)$ is the occupation number of jth intramolecular phonon mode with frequency ω_j, and S_j is the Huang-Rhys factor measuring the coupling strength between the carrier on-site energy and the jth phonon mode, which is kept constant during the Monte-Carlo simulation. The low frequency lattice modes are neglected in eqn (4) since they are less coupled to the on-site energies than intramolecular vibrations.[16] Note that V in eqn (4) can be treated as a constant, which lies in the fact that the charge transfer time between a dimer in this system (a few to tens of femtoseconds, see below) is much less than the transfer integral fluctuating period (*e.g.*, 667 fs for 50 cm^{-1}, see below).

E Kinetic Monte-Carlo simulation

Given the Huang-Rhys factors and the Fourier coefficients for transfer integrals of typical dimers, the kinetic Monte-Carlo simulation containing dynamic disorder effects can be performed using the quantum charge transfer rates. We create the system with periodic boundary condition and choose one molecule as the starting charge center. For each molecular dimer, the initial phase factor φ_0 in eqn (3) is chosen randomly as $r\omega_k t_\mathrm{simu}$, where r is uniformly distributed in [0,1] and t_simu is the total MD simulation time. The hopping rates for the charge at site m to all its neighbors are calculated using eqn (4). Then the hopping probability for the charge to the nth neighbor is $P_{mn} = k_{mn}/\Sigma_{n'}k_{mn'}$. After determining the next position for the charge, the Monte-Carlo simulation time is incremented by $1/\sum_{n'}k_{mn'}$ and the transfer integrals are updated using eqn (3) for the new time. The simulation continues until the total simulation time is achieved. Such simulations are repeated to get thousands of independent charge diffusion trajectories, then the averaged squared displacement reaches a linear function as simulation time. Finally, the diffusion coefficient $D = \langle l^2\rangle/(2t)$ can be obtained (see Fig. 2) and the charge mobility is evaluated through the Einstein formula $\mu = eD/k_\mathrm{B}T$. Note that the statistical error of the simulated mobility can be evaluated using a simplified process proposed in our previous work.[22,43]

III. Results and discussion

A Computational details

A 3 × 3 × 3 supercell is chosen and depicted in Fig. 3 based on the crystal structure.[46] The MD simulation with fixed lattice constants is carried out at five constant temperatures, *i.e.*, 100, 150, 200, 250 and 300 K with COMPASS force field within the Materials Studio package.[47] In order to ensure the validity of COMPASS force field in the present system, we perform another MD simulation to the crystal in NPT ensemble at 300 K and ambient pressure. We find that the lattice constants

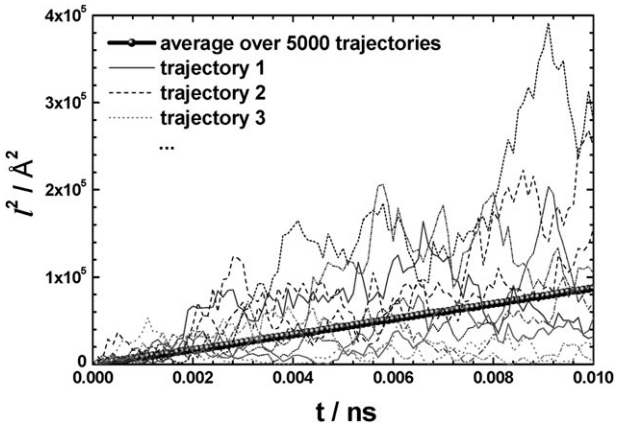

Fig. 2 Squared displacement *versus* simulation time for a 2-D pentacene layer with dynamic disorder at 300 K. Each thin solid line represents an individual trajectory of the kinetic Monte-Carlo simulation. The thick dotted line means the average over 5000 independent trajectories.

fluctuate around the experimental value, *e.g.*, the mean lattice constant a is 5.962 Å, which is very close to the experimental value of 5.958 Å. After a further geometry optimization with fixed lattice, detailed comparison of the bond lengths, bond angles, and intermolecular relative orientations are shown in Table 1, from which very small differences can be observed. Furthermore, the normal mode analysis is performed with molecular mechanics. We find that there are only four lattice modes with frequencies smaller than 50 cm^{-1} which are important to the fluctuation of transfer integrals, and two of them are Raman active modes with frequencies of 23 and 31 cm^{-1}, respectively. Very recently, highly uniform monolayers of pentacene have been deposited on polymeric substrate which enables the observation of low-lying lattice modes of pentacene thin film phase using Raman spectra to characterize the intermolecular vibration.[48] The first two peaks in the spectra correspond to frequencies of 28 and 33 cm^{-1}. Therefore, the COMPASS force field also gives a very good description of the lattice modes which are very important to the dynamic disorder in this study. The Berendsen thermostat is chosen to simulate constant temperatures.[49] The simulation time is set to be 100 ps with a time step of 2 fs, and the dynamic trajectories are extracted every 30 fs after thermal equilibration of 40 ps with a total number of 2000 snapshots. Within one layer, each molecule has six nearest neighbors. From the symmetry, we only calculate the transfer integrals for typical molecular dimers *A*, *B*, and *C* (see Fig. 3). The electronic structures of single molecules and molecular dimers are calculated using Gaussian 03 package with the PW91PW91 exchange–correlation functional and a 6-31G* basis set.[50] The simulation time for a single kinetic Monte-Carlo is 10 ps and 5000 simulations are performed to get carrier mobility.

B Transfer integral fluctuation

As shown in Fig. 4a, the thermal fluctuation of the transfer integrals are found to be of the same order of magnitude as the average value, agreeing with the observations in other

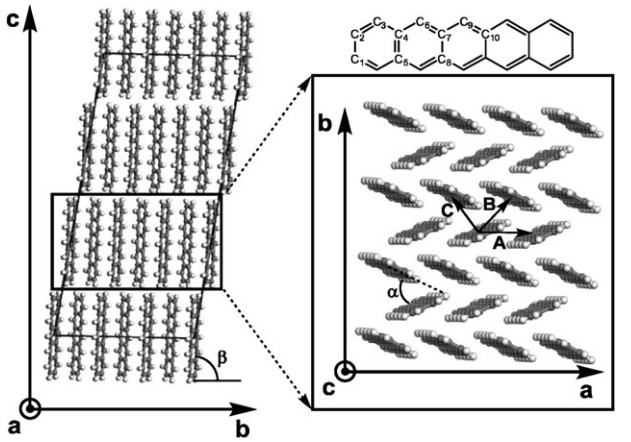

Fig. 3 (Left) A 3 × 3 × 3 supercell structure of pentacene crystal of thin film phase; (right) an *a*–*b* plane extracted from the supercell. The three arrows indicate three typical dimers *A*, *B*, and *C*. The chemical structure of pentacene is shown. α is the dihedral angle between two intra-layer molecules, and β is the tilt angle of the molecules with respect to the layer plane.

Table 1 Comparison of molecular geometries between MD simulation (NPT ensemble at 300 K and ambient pressure using COMPASS force field) and the experimental data.[46]

	Experiment	Calculation	Difference
C_1C_2	1.45 Å	1.40 Å	−0.05 Å
C_2C_3	1.35 Å	1.38 Å	0.03 Å
C_3C_4	1.44 Å	1.42 Å	−0.02 Å
C_4C_5	1.44 Å	1.45 Å	0.01 Å
C_4C_6	1.38 Å	1.40 Å	0.02 Å
C_6C_7	1.40 Å	1.40 Å	0.00 Å
C_7C_8	1.46 Å	1.45 Å	−0.01 Å
C_7C_9	1.41 Å	1.40 Å	−0.01 Å
$C_1C_2C_3$	120.2°	120.6°	0.4°
$C_2C_3C_4$	121.4°	120.7°	−0.7°
$C_3C_4C_5$	119.3°	118.7°	−0.6°
$C_5C_4C_6$	119.7°	119.4°	−0.3°
$C_4C_6C_7$	121.7°	121.4°	−0.3°
$C_6C_7C_8$	118.6°	119.3°	0.7°
$C_8C_7C_9$	118.9°	119.2°	0.3°
$C_7C_9C_{10}$	122.2°	121.6°	−0.6°
α	54.3°	53.2°	−1.1°
β	86.5°	87.4°	0.9°

polymorph of pentacene crystals.[19] Besides, they follow the Gaussian distributions with almost temperature-independent mean values (Fig. 4b), and the square of the standard deviation, σ_V^2, is a linear function of temperature (Fig. 4c), which can be understood by the combined effects of Boltzmann distribution of the intermolecular distances and the widely assumed linear electron–phonon coupling.[14] Accordingly, the Fourier coefficients should also follow the $T^{0.5}$ law like σ_V with temperature and then the coefficients at any temperature can be evaluated from that in 300 K. From Fig. 4d, we can find that the major contribution to the transfer integral fluctuation comes from the low frequency phonon modes (<50 cm^{-1}), belonging to the intermolecular vibrations. Here we have not considered the quantum sampling which is important at very low temperatures.[51]

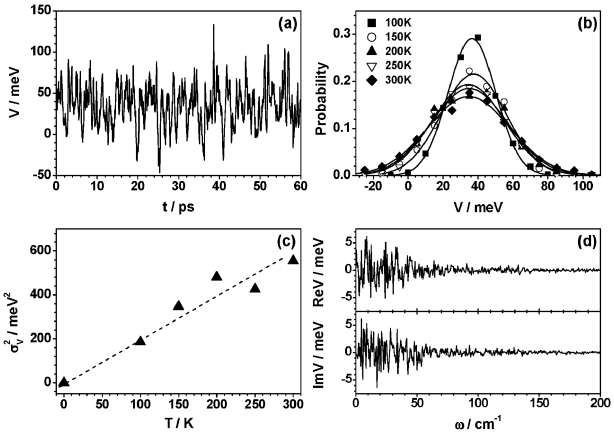

Fig. 4 (a) Thermal fluctuation of the transfer integral (dimer *A*) at 300 K; (b) distribution of the transfer integrals at different temperatures; (c) square of the standard deviation of transfer integrals *vs.* temperature, where σ_V is set to zero at zero temperature in the classical limit; and (d) Fourier transformation of thermal deviation amplitude (ReV and ImV) at 300 K.

C Mobility calculation

We first consider a 1-D stacked chain along the *a* axis (Fig. 3) containing 100 molecules in one supercell with a periodic boundary. A different system size has been tested and negligible size effect on the mobility has been found (Table 2). The temperature dependent hole mobility both with and without thermal fluctuation is calculated and displayed in Fig. 5. Mobility decreases with temperature in both cases, agreeing well with previous studies based on solving self-consistently the time-dependent Schrödinger equation associated with the semiclassical Hamiltonian.[14] Due to the fluctuating nature of the transfer integral, the charge transfer rates between parts of the molecular dimers become less than those at the equilibrium geometry. Then in 1-D, these dimers become bottle necks for charge transport. Namely, the charge becomes oscillating between dimers with larger charge transfer rate, and the overall diffusion constant is reduced. It is noted that even at low temperature (100 K), the disorder effect is remarkable. This is due to the fact that the dominant intermolecular mode is around 50 cm^{-1}, which can be converted to about 72 K. The ratio between the simulated mobility with and without dynamic disorder decreases with temperature due to the larger fluctuation of transfer integrals and thus more pronouced "bottleneck effect" at higher temperatures (Fig. 5).

Then, we come to the 2-D molecular monolayer with periodic boundary conditions along both *a* and *b* axes. The numerical results show that the temperature dependence of the mobility does not depend on the dynamic disorder for a wide range of temperatures, see Fig. 5, which is in sharp contrast to the 1-D case. Within the layer, there are much more hopping pathways in 2-D than in 1-D case. If the transfer integral of one path is small, the hole can always choose other pathways with large transfer integrals, then the hole diffusion is much less affected by the thermal fluctuation as seen in 1-D. Thus, the "band-like" behavior of mobility in 2-D is purely a nuclear tunneling effect observed with static transfer integrals.[22] In this case, the charge transfer rates are independent of temperature

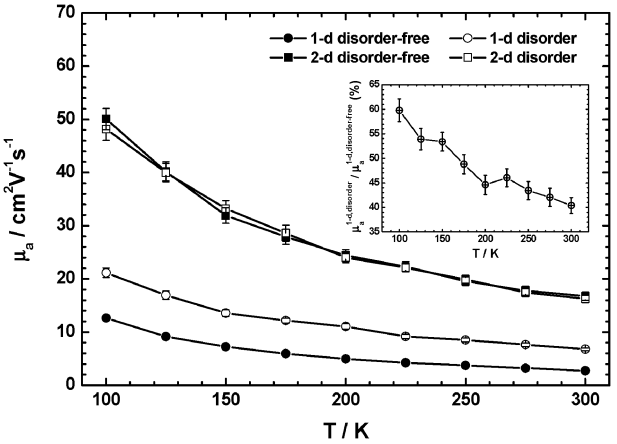

Fig. 5 Temperature dependent hole mobility along the *a* axis with and without dynamic disorder in 1-D (circles) and 2-D (squares). The ratio between the mobility with and without dynamic disorder in 1-D is shown in the inset.

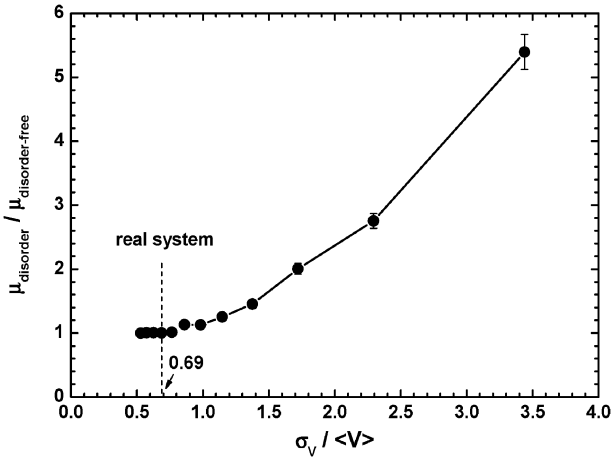

Fig. 6 Ratio of the hole mobility along *a* axis in 2-D with dynamic disorder with respect to that of disorder-free, as a function of the standard deviation of the transfer integrals (σ_V) over the mean transfer integral ($\langle V\rangle$). Here, σ_V is kept at the value in 300 K, while $\langle V\rangle$ is varied. The dashed bar indicates the value in the actual pentacene thin film phase. The phonon-assisted current starts at about $\sigma_V/\langle V\rangle = 1$.

bellow room temperature and govern the overall temperature dependence of mobility. The room temperature mobility is calculated to be around 17 $cm^2\ V^{-1}\ s^{-1}$ which is reasonably comparable to the available experimental measurement of over 5 $cm^2\ V^{-1}\ s^{-1}$.[24]

If we go to an extreme case where the fluctuation in transfer integral is even larger than its average, for instance, by keeping the same σ_V and reducing the average $\langle V\rangle$, which is possible for more floppy molecules, we find that the dynamic disorder can even increase the hole mobility for 2-D (Fig. 6). This indicates a transition to the phonon-assisted transport behavior by dynamic disorder, as has been found in a small polaron model by Munn and Silbey.[15] According to our study, the critical value for $\sigma_V/\langle V\rangle$ is around 1.

To reveal the dimension dependence of disorder effects on the transport behavior, we define two quantities: $R = \langle l^2\rangle/n$, the average squared diffusion length per hopping step and $\tau = t/n$, the average time per hopping step. Then the diffusion constant is expressed as $D = R/(2\tau)$. Both R and τ decrease with dynamic disorder: the former is reduced because of the barriers caused by dimers with smaller hopping rates, while the latter decreases because of the increase in the average hopping rate. If we take a look at Fig. 4b, the electronic coupling is Gaussian distributed. According to eqn (4), the average hopping rate is proportional to the $\langle V^2\rangle$, which is equal to $\langle V\rangle^2 + \sigma_V{}^2$, namely always larger than $\langle V\rangle^2$. Then, the hopping time is decreased since it is proportional to $1/\langle V^2\rangle$. For the 1-D case, R decreases from 34.50 $Å^2$ (disorder free case) to 9.44 $Å^2$ with disorder at room temperature and meanwhile τ is only decreased from 9.87 to 6.67 fs. As a result, the overall ratio R/τ is decreased by the disorder, see Fig. 7. However, for 2-D, R and τ decrease from 13.38 $Å^2$ and 1.55 fs to 10.60 $Å^2$ and 1.22 fs, respectively, leaving their ratio almost unchanged (Fig. 7). Here, we consider only the mobility along the *a*-axis. Thus, for the 2-D case, when a projection to the *a*-axis is made, the 2-D R value becomes smaller than the 1-D case. The intermolecular charge transfer time τ is indeed very small (a few fs), which arises from the large intermolecular transfer integrals and the small Huang-Rhys factors for pentacene. That the resulting mobility is in good agreement with the experiment indicates such a time scale is reasonable.

At last, the present approach in dealing with dynamic disorder is based on the precondition that the fluctuation of the transfer integrals is much slower than the charge transfer process along individual molecular dimers. When the transfer integrals are too small, for instance, when dealing the interlayer coupling, the evaluation of the dynamic disorder effect to charge transport poses a lot of difficulties, which deserves further exploration. However, going from 2-D to 3-D would not change the physical picture at all.

IV. Conclusion

To summarize, we apply a multiscale approach combining molecular dynamics, quantum mechanics and kinetic Monte-Carlo simulations to study the dynamic disorder effect on charge transport in organic semiconductors. We find that the dynamic disorder drastically reduces the charge mobility for

Table 2 Simulated room temperature (300 K) hole mobility for 1-D pentacene stacking array and 2-D herringbone layer with different supercell size under periodic boundary condition. Negligible effect of the system size to the simulated mobility can be observed when considering the error of the kinetic Monte-Carlo simulations (about 5% of the averaged mobility with 5000 trajectories)

Size	1-D mobility/$cm^2\ V^{-1}\ s^{-1}$	Size	2-D mobility/$cm^2\ V^{-1}\ s^{-1}$
10	2.92 ± 0.13	10 × 10	16.72 ± 0.72
50	2.82 ± 0.11	50 × 50	17.17 ± 0.81
100	2.73 ± 0.11	100 × 100	16.75 ± 0.75

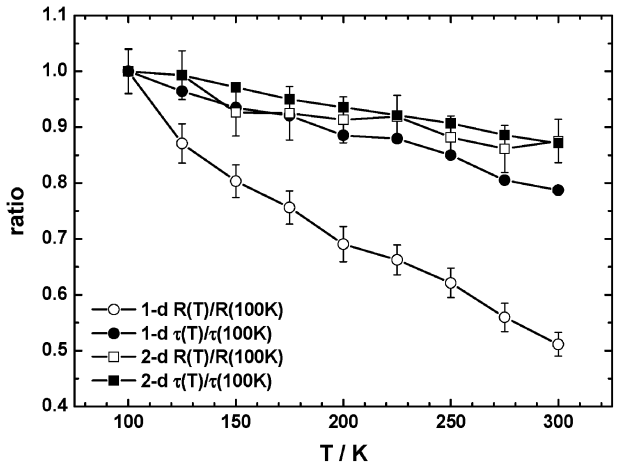

Fig. 7 Temperature dependence of the two quantities $R(T)$ and $\tau(T)$ which are normalized to the values in 100 K in 1-D (circles) and 2-D (squares).

1-D molecular arrays, but has no significant influence in the 2-D case. We conclude that the previously proposed "band-like" transport behavior in organic semiconductor is due neither to the band-like behavior nor to the disorder-induced decrease in mobility. Instead, it is due to the "nuclear tunneling" effect of intramolecular vibrations in the quantum charge transfer process. When the mean transfer integral becomes less than its standard deviation, the dynamic disorder even tends to enhance the charge mobility for 2-D.

Acknowledgements

This work is supported by the National Science Foundation of China (Grant Nos. 20833004, 20773145 and 20733006), the Ministry of Science and Technology of China (Grant Nos. 2006CB806200, 2006CB932100, and 2009CB623600), as well as by the EU project "MODECOM".

References

1 A. R. Murphy and J. M. J. Fréchet, *Chem. Rev.*, 2007, **107**, 1066.
2 J. E. Anthony, *Angew. Chem., Int. Ed.*, 2008, **47**, 452.
3 M. Mas-Torrent and C. Rovira, *Chem. Soc. Rev.*, 2008, **37**, 827.
4 M. E. Gershenson, V. Podzorov and A. F. Morpurgo, *Rev. Mod. Phys.*, 2006, **78**, 973.
5 V. Coropceanu, J. Cornil, D. A. da Silva Filho, Y. Olivier, R. Silbey and J. L. Brédas, *Chem. Rev.*, 2007, **107**, 926.
6 D. L. Cheung and A. Troisi, *Phys. Chem. Chem. Phys.*, 2008, **10**, 5941.
7 J.-L. Brédas, D. Beljonne, V. Coropceanu and J. Cornil, *Chem. Rev.*, 2004, **104**, 4971.
8 N. Karl, *Synth. Met.*, 2003, **133–134**, 649.
9 V. Podzorov, E. Menard, A. Borissov, V. Kiryukhin, J. A. Rogers and M. E. Gershenson, *Phys. Rev. Lett.*, 2004, **93**, 086602.
10 O. D. Jurchescu, J. Baas and T. T. M. Palstra, *Appl. Phys. Lett.*, 2004, **84**, 3061.
11 O. Ostroverkhova, D. G. Cooke, F. A. Hegmann, J. E. Anthony, V. Podzorov, M. E. Gershenson, O. D. Jurchescu and T. T. M. Palstra, *Appl. Phys. Lett.*, 2006, **88**, 162101.
12 V. Podzorov, E. Menard, J. A. Rogers and M. E. Gershenson, *Phys. Rev. Lett.*, 2005, **95**, 226601.
13 Y. C. Cheng, R. J. Silbey, D. A. da Silva Filho, J. P. Calbert, J. Cornil and J. L. Brédas, *J. Chem. Phys.*, 2003, **118**, 3764.
14 A. Troisi and G. Orlandi, *Phys. Rev. Lett.*, 2006, **96**, 086601.
15 R. W. Munn and R. Silbey, *J. Chem. Phys.*, 1985, **83**, 1854.
16 L. J. Wang, Q. Peng, Q. K. Li and Z. Shuai, *J. Chem. Phys.*, 2007, **127**, 044506.
17 K. Hannewald and P. A. Bobbert, *Appl. Phys. Lett.*, 2004, **85**, 1535.
18 L. J. Wang, Q. K. Li and Z. Shuai, *J. Chem. Phys.*, 2008, **128**, 194706.
19 A. Troisi and G. Orlandi, *J. Phys. Chem. A*, 2006, **110**, 4065.
20 E. Abrahams, P. W. Anderson, D. C. Licciardello and T. V. Ramakrishnan, *Phys. Rev. Lett.*, 1979, **42**, 673.
21 S. Sarker and E. Domany, *Phys. Rev. B: Condens. Matter*, 1981, **23**, 6018.
22 G. J. Nan, X. D. Yang, L. J. Wang, Z. Shuai and Y. Zhao, *Phys. Rev. B: Condens. Matter Mater. Phys.*, 2009, **79**, 115203.
23 K. Hannewald, V. M. Stojanović, J. M. T. Schellekens and P. A. Bobbert, *Phys. Rev. B: Condens. Matter Mater. Phys.*, 2004, **69**, 075211.
24 T. W. Kelley, D. V. Muyres, P. F. Baude, T. P. Smith and T. D. Jones, *Mater. Res. Soc. Symp. Proc.*, 2003, **771**, L6.5.
25 D. Nabok, P. Puschnig, C. Ambrosch-Draxl, O. Werzer, R. Resel and D. Smilgies, *Phys. Rev. B: Condens. Matter Mater. Phys.*, 2007, **76**, 235322.
26 P. Parisse, S. Picozzi, M. Passacantando and L. Ottaviano, *Thin Solid Films*, 2007, **515**, 8316.
27 M. Kitamura and Y. Arakawa, *J. Phys.: Condens. Matter*, 2008, **20**, 184011.
28 W. M. Young and E. W. Elcock, *Proc. Phys. Soc.*, 1966, **89**, 735.
29 B. Kramer and A. MacKinnon, *Rep. Prog. Phys.*, 1993, **56**, 1469.
30 P. W. Anderson, *Phys. Rev.*, 1958, **109**, 1492.
31 F. C. Grozema and L. D. A. Siebbeles, *Int. Rev. Phys. Chem.*, 2008, **27**, 87.
32 J. R. Reimers, *J. Chem. Phys.*, 2001, **115**, 9103.
33 G. R. Hutchison, M. A. Ratner and T. J. Marks, *J. Am. Chem. Soc.*, 2005, **127**, 16866.
34 J. Cornil, D. Beljonne, J.-P. Calbert and J.-L. Brédas, *Adv. Mater.*, 2001, **13**, 1053.
35 X. Y. Li, *J. Comput. Chem.*, 2001, **22**, 565.
36 T. Fujita, H. Nakai and H. Nakatsuji, *J. Chem. Phys.*, 1996, **104**, 2410.
37 A. Troisi and G. Orlandi, *Chem. Phys. Lett.*, 2001, **344**, 509.
38 E. F. Valeev, V. Coropceanu, D. A. da Silva Filho, S. Salman and J. L. Brédas, *J. Am. Chem. Soc.*, 2006, **128**, 9882.
39 G. J. Nan, L. J. Wang, X. D. Yang, Z. Shuai and Y. Zhao, *J. Chem. Phys.*, 2009, **130**, 024704.
40 R. A. Marcus, *Rev. Mod. Phys.*, 1993, **65**, 599.
41 J.-L. Brédas, J. P. Calbert, D. A. da Silva Filho and J. Cornil, *Proc. Natl. Acad. Sci. U. S. A.*, 2002, **99**, 5804.
42 X. D. Yang, Q. K. Li and Z. Shuai, *Nanotechnology*, 2007, **18**, 424029.
43 X. D. Yang, L. J. Wang, C. L. Wang, W. Long and Z. Shuai, *Chem. Mater.*, 2008, **20**, 3205.
44 V. Coropceanu, R. S. Sánchez-Carrera, P. Paramonov, G. M. Day and J.-L. Brédas, *J. Phys. Chem. C*, 2009, **113**, 4679.
45 S. H. Lin, C. H. Chang, K. K. Liang, R. Chang, Y. J. Shiu, J. M. Zhang, T. S. Yang, M. Hayashi and F. C. Hsu, *Adv. Chem. Phys.*, 2002, **121**, 1.
46 S. Schiefer, M. Huth, A. Dobrinevski and B. Nickel, *J. Am. Chem. Soc.*, 2007, **129**, 10316.
47 H. Sun, *J. Phys. Chem. B*, 1998, **102**, 7338.
48 R. He, N. G. Tassi, G. B. Blanchet and A. Pinczuk, *Appl. Phys. Lett.*, 2009, **94**, 223310.
49 H. J. C. Berendsen, J. P. M. Postma, W. F. van Gunsteren, A. DiNola and J. R. Haak, *J. Chem. Phys.*, 1984, **81**, 3684.
50 M. J. Frisch, *et al.*, *GAUSSIAN 03 (Revision E01)*, Gaussian Inc., Wallingford, CT, 2004.
51 J. J. Kwiatkowski, J. M. Frost, J. Kirkpatrick and J. Nelson, *J. Phys. Chem. A*, 2008, **112**, 9113.

